



Published in final edited form as:

*Ann Thorac Surg.* 2021 October ; 112(4): 1150–1159. doi:10.1016/j.athoracsur.2020.09.037.

## Multi-Institutional Phase 2 Clinical Trial of Intraoperative Molecular Imaging of Lung Cancer

Sidhu Gangadharan, MD<sup>1,\*</sup>, Inderpal Sarkaria, MD<sup>2,\*</sup>, David Rice, MD<sup>3</sup>, Sudish Murthy, MD<sup>4</sup>, Jerry Braun, MD<sup>5</sup>, John Kucharczuk, MD<sup>6</sup>, Jarrod Predina, MD<sup>6</sup>, Sunil Singhal, MD<sup>6</sup>

<sup>1</sup>Beth Israel Deaconess

<sup>2</sup>University of Pittsburgh

<sup>3</sup>MD Anderson

<sup>4</sup>Cleveland Clinic

<sup>5</sup>Leiden University

<sup>6</sup>University of Pennsylvania

### Abstract

**Background:** Intraoperative molecular imaging (IMI) may improve surgical outcomes during pulmonary resection for lung cancer. A multi-institutional Phase 2 IMI clinical trial was conducted utilizing a near-infrared (NIR), folate-receptor targeted contrast agent for lung adenocarcinomas, OTL38. The primary goal was to determine if OTL38 improved surgeons' ability to identify hard-to-find nodules, occult cancers, and positive margins.

**Methods:** Patients with lung nodules received OTL38 (0.025mg/kg) preoperatively. Patients had IMI sequentially during lung inspection, tumor resection, and margin check. Efficacy was evaluated by occurrence of clinically significant events (CSE), occurrences that caused the surgeon to modify the operation or up-stage the patient's cancer. Safety was assessed for single intravenous dose of OTL38.

**Results:** Of 110 patients recruited; 92 were eligible for analysis. During Lung Inspection, IMI found 24 additional nodules, 9 (10%) of which were cancers that had not been known preoperatively. During Tumor Resection, IMI located 11 (12%) lesions that the surgeon could not find. During Margin Check, IMI revealed 8 positive margins (9%) that the surgeon thought was negative. Benefits of IMI were pronounced in patients undergoing sublobar pulmonary resections and in those with ground-glass opacities. There were no serious adverse events. All surgeons felt comfortable with the procedures by 10 cases.

---

**Corresponding author:** Sunil Singhal, MD, Associate Professor, University of Pennsylvania School of Medicine, Department of Surgery, 6 Silverstein Pavilion, 3400 Spruce Street, Philadelphia, PA 19104, sunil.singhal@uphs.upenn.edu.

\*These authors contributed equally

**Publisher's Disclaimer:** This is a PDF file of an unedited manuscript that has been accepted for publication. As a service to our customers we are providing this early version of the manuscript. The manuscript will undergo copyediting, typesetting, and review of the resulting proof before it is published in its final form. Please note that during the production process errors may be discovered which could affect the content, and all legal disclaimers that apply to the journal pertain.

**Conclusions:** In this Phase 2 clinical trial, IMI improved outcomes for 26% of patients. A randomized, multi-institutional Phase 3 clinical trial is underway.

[CLINICALTRIALS.GOV](https://clinicaltrials.gov/ct2/show/study/NCT02872701) — NCT02872701

### Keywords

Surgery; Molecular imaging; Folate receptor; Clinical trial

---

Pulmonary resection is recommended for most patients who have Stage I-II non-small cell lung cancer (NSCLC). The goal is complete resection, minimize unnecessary resections, and accurate staging. Challenges include identification of small nodules, recognition of synchronous cancers or advanced cancers, and confirmation of negative margins. These challenges are magnified because of increasing use of minimally invasive surgery where tactile feedback is reduced and chest assessment is compromised.

One decade ago, our group introduced intraoperative molecular imaging (IMI) to improve outcomes in lung cancer surgery (1–11). It requires (i) a fluorescent optical dye that is delivered systemically prior to surgery and that selectively targets tumors and the microenvironment, and (ii) an imaging system to detect the dye in the tumor. It does not involve ionizing radiation, thus eliminating exposure risks to both patient and surgeon. Because the tracer is administered intravenously, tumor-specific accumulation allows for identification of otherwise unknown and unrecognized lesions with no *a priori* knowledge of the presence or location of the cancer. The targeted nature of IMI permits post-resection analysis helpful in evaluating resection margins. Back-table imaging adds less than 5 minutes to the case(10, 12). Logistically, injected a contrast agent into the patient does not disrupt the surgical flow.

We have developed and investigated 3 fluorescent dyes in over 600 patients with thoracic malignancies (lung cancer, thymoma, mesothelioma, germ cell tumor, metastatic sarcoma, metastatic colorectal cancer): TumorGlow, EC17, and OTL38 (7, 8, 12–22). The most promising tracer for lung adenocarcinomas and ground glass opacities is OTL38, for which we recently reported pilot and Phase I data(11). OTL38 targets the folate receptor alpha (FR $\alpha$ ) which is expressed in 90 – 95% of lung adenocarcinomas and in ground glass opacities(9, 21, 23). Folate receptor alpha is highly expressed ( $10^3$ – $10^4$  receptors/cell) on lung adenocarcinomas compared to surrounding normal lung parenchyma(24). The near-infrared dye emits at 795nm so it is not visible to the naked eye but can be seen with a thoracoscope which gives 2 cm depth of penetration into the lung.

We conducted an open-label multi-institutional Phase 2 clinical trial to assess the role of IMI in patients undergoing standard-of-care pulmonary resection. Efficacy was evaluated by occurrence of clinically significant events (CSE); we defined a CSE as any occurrences that causes the surgeon to modify the operation, identify additional cancers and/or up-stage the patient's cancer.

## Patients and Methods

### Design

Our Phase 2 clinical trial ([NCT02872701](#), PI: Singhal) was approved by the six Institutional Review Boards (Beth Israel Deaconess, University of Pittsburgh, MD Anderson, Cleveland Clinic, Leiden University, University of Pennsylvania). Patients provided informed consent and underwent CT scanning with 1 mm slice thickness and standard evaluations at the discretion of the surgeon (e.g. PET, pulmonary function tests, biopsy). Study participants received 0.025 mg/kg of intravenous OTL38 through a peripheral vein 2 to 6 hours prior to resection. Patients were assessed sequentially during (a) Lung Inspection, (b) Tumor Resection, and (c) Margin Check. In each situation, the surgeon first performed the standard-of-care. Then, the surgeon used IMI to look for additional cancer. Thus, each patients served as their own control subject. If the surgeon changed the operation because of a finding discovered by IMI, the finding was designated a CSE.

We performed the operation in three standard steps (Figure 1). First, during Lung Inspection, the surgeon entered the chest by robotic, video-assisted thoracoscopic surgery (VATS) or thoracotomy, then surveyed for additional tumors by visual inspection or palpation. Then, IMI was used to find additional nodules. If discovered, the surgeon decided whether the nodule could be resected safely without significantly changing the operation.

Second, during Tumor Resection, the surgeon performed the standard-of-care removal of the known primary pulmonary nodule and lymph node dissection. The surgeon utilized white-light and manual palpation through the port-site incisions to confirm the location of the lesion. Only if the surgeon could not find the nodule, IMI was used to help locate the lesion.

Third, after the specimen was removed, it was examined on the back table to assess the margins. A positive margin was arbitrarily defined as fluorescence within 5 mm of the parenchymal staple line. The specimen was submitted for pathologic examination by a specialized lung pathologist. A portion of the specimen was sent to a central pathology core where 2 blinded pathologists independently assessed each sample.

All excised specimens were examined using standard hematoxylin/eosin staining. Additionally, immunohistochemical staining for FR $\alpha$  was performed using a monoclonal antibody, Biocare Medical BRI4006KAA. For immunohistochemistry, human kidney, with primary antibody and without primary antibody applied, were used as positive and negative controls, respectively. Only nodules or margins that are fluorescent and contain cancer cells were “true positives”. Any nodules or margins that were fluorescent but did not contain cancer cells were “false positives”.

### Molecular contrast agent

OTL38 (chemical formula:  $C_{61}H_{63}N_9Na_4O_{17}S_4$  (tetrasodium salt); molecular weight: 1414.42 Da) is a folate analogue conjugated to a near-infrared (NIR) fluorescent contrast agent. OTL38 maximally excites at a wavelength of 774–776 nm and has a peak emission

of 794–796 nm<sup>(23)</sup>. OTL38 (>99% purity) was obtained from On Target Laboratories (West Lafayette, IN).

### NIR camera

In situ, real-time fluorescent imaging was performed using one of 4 camera systems: Quest Artemis, Medtronic VisionSense3, Stryker AIM-C1, and Olympus IR-C0003. No institution had access to all the cameras, and each case was imaged using only one camera system. The design of all systems is essentially the same: An excitation source with a wavelength of ~785nm (range 750–785nm) was used to excite the fluorophore. Then a detector would selectively filter light outside the 800–835nm range. For correlative studies, back-table specimen analysis was performed using either a Medtronic VisionSense3 exoscope, LiCor ELVIS prototype, or Odyssey flat-bed scanner.

### Qualification of fluorescence

Similar to the concept of a standardized uptake value (SUV) for PET scanning, we developed a tumor-to-background ratio (TBR): Mean Fluorescence Intensity of the tumor ( $MFI_{\text{tumor}}$ ) was obtained by analyzing monochromatic NIR images with ImageJ(<http://rsb.info.nih.gov/ij>). Background fluorescence (0.5–1.0cm from margin) was obtained ( $MFI_{\text{background}}$ ), with a minimum of 1000 pixels from surrounding normal lung. Calculations were repeated in triplicate from varying angles and calculated:

$$TBR = \frac{MFI_{\text{Tumor}}}{MFI_{\text{Background}}}$$

A mean TBR >2.0 was considered fluorescent.

### Statistical Analysis

The primary objective of this study was to evaluate the role of OTL38 used with NIR fluorescent imaging to detect 1 of the following outcomes in patients undergoing pulmonary resection:

- a. 1 primary cancerous nodule not detected visually and/or with palpation; or
- b. 1 cancerous synchronous lesion not detected visually and/or with palpation; or
- c. Identification of a cancer-positive margin by fluorescence 5 mm from the staple line.

Any one of these findings qualified as a CSE. Safety was assessed using standard guidelines ([https://ctep.cancer.gov/protocolDevelopment/electronic\\_applications/ctc.htm](https://ctep.cancer.gov/protocolDevelopment/electronic_applications/ctc.htm)). A point estimate along with a 95% confidence interval (CI) was provided for CSE rate. The CI was calculated using the exact binomial distribution.

## Results

### Patient Characteristics

One hundred patients received the drug and patient characteristics are described in Table 1 and the Figure 2.

### Safety Profile

Twenty patients experienced drug-related adverse events, all during the infusion: 12 Grade I, 6 Grade II, and 2 Grade III, with no serious adverse events. Most events were a sensation of nausea. The two primary drug-related toxicities were a report of chest pain (normal EKG and troponins) and an oxygen desaturation (resolved by terminating infusion). All reactions responded to slowing or interrupting the infusion or other intervention (diphenhydramine, famotidine, ondansetron). None had sequelae.

### Lung Inspection

Intraoperative molecular imaging found 9 additional cancers (9.8%) in 92 patients, thereby changing the stage of 7 patients (7.6%).

Without IMI, the surgeons found 2 additional nodules in 92 patients (metastatic colorectal cancer and granuloma). Then IMI identified an additional 24 pulmonary nodules. All these nodules were felt to be safe to remove with a wedge and did not require an anatomical resection.

Of the 24 synchronous nodules that were removed, 9 were occult cancers. These 9 lesions were discovered within 7 patients (2 patients with multiple additional malignancies). The histology of these 9 cancers included primary adenocarcinomas (n=6), metastatic papillary thyroid cancer (n=2), and adenoid cystic carcinoma (n=1). The addition of these lesions upstaged each patient (7 Stage IA NSCLC, 1 Stage III NSCLC, 1 Stage IV papillary thyroid cancer). Representative examples where IMI identified a synchronous lesion are shown in Figure 3.

The 15 synchronous non-cancerous lesions were inflamed parietal pleural and pericardial fragments (n=4), granulomas (n=3), adenomatous atypical hyperplasia (n=2), meningiothelioid tissue (n=2), undefined lesion, organizing pneumonia, a microcoil, sclerosing tissue, and a hamartoma.

### Tumor Resection

Surgeons successfully localized 79 out of the 92 preoperatively identified pulmonary nodules by traditional white-light visualization or manual palpation. In the remaining 13 cases, the surgeon could not locate the primary tumor (Figure 4). Eleven nodules were found by IMI, mean size was 1.54cm versus 2.27cm for all the nodules in the study. Mean distance from the surface of the nodules found by NIR imaging was 6mm (range 0–14mm). Identification of these lesions allowed a wedge resection for diagnosis prior to an anatomical resection. In one case, the wedge proved the nodule was not cancer and saved the patient further surgery. In the remaining two non-localized cases, the surgeons either performed a

lobectomy or a thoracotomy to locate the nodule. Patients with difficult-to-palpate GGOs had particular benefit from IMI (6 of 11 cases).

### Margin Check

FR-IMI provided real-time feedback to the surgeon regarding margin status. *In vivo*, surgeons were asked to subjectively record if their operation was altered based on IMI. In no cases had the surgeon modified placement of the stapler because of the concern of a close surgical margin.

*Ex vivo*, the surgeons inspected the specimen on the back table. Without IMI, the surgeons felt all cases had a negative margin. With IMI, 16 patients had fluorescence within 5mm of the staple line (Figure 5). On final pathology, 9 of the 16 parenchymal margins were positive for cancer.

Incorporation of this information into the resection algorithm provided reliable, real-time feedback resulting in immediate re-resection in five of the 9 positive margins. In one situation, the surgeon chose not to act upon the IMI data. In 3 cases, the surgeon was satisfied because a lobectomy had been performed and considered the 5 mm margin sufficient.

### Subgroup Analysis

Patients undergoing a sublobar resection benefitted more than patients undergoing a lobectomy. The total number of CSEs in lobar patients was 8 in 44 patients (18%). Out of 52 sublobar resections, 16 patients (31%) each had a CSE.

First, those patients undergoing a sublobar resection had the highest proportion of positive margins. Second, in those cases, the surgeon was unable to find the nodule in 5 of the 52 cases. In these instances, the surgeons had the option of a larger resection with the intent of including the nodule, thoracotomy, or lobectomy. In all 5 of these sublobar resections, IMI found the nodule. This allowed the surgeon to complete the intended operation without escalating the procedure.

### Learning Curve

We surveyed the surgeons (n=7) in the group. IMI took on average 15 minutes, with a trend towards less time as the surgeon gained experience. Except for 2 surgeons who had previously performed several cases prior to the Phase 2, most of the surgeons had not used IMI. The mean number of cases required prior to developing comfort with the machine and the image quality was 6, and all surgeons felt comfort by 10 cases.

### Overall Results

Twenty-eight CSEs were noted among 24 patients (26%) of 92 patients (4 patients experienced 2 or more CSEs). The results are summarized in Table 2 and Figure 6.

## Comment

Over the last 30 years, thoracic surgeons have made significant advancements in the technical aspects of surgery for lung cancer. Difficulties remain in localizing small synchronous lesions, finding ground glass opacities and in assessing margins. We introduced IMI as a novel intraoperative tool that augments the surgeon's ability to identify tumor deposits beyond visual and tactile feedback (7, 8, 12–22).

Over the last decade, we showed that targeted contrast agents can bind various lung tumors both in-vitro and in in-vivo animal models(3, 21). Intraoperative molecular imaging can identify as few as  $10^4$  cancer cells and can locate nodules as small as 0.5 mm in laboratory conditions. In follow-up studies, IMI was reliable at detecting nodules during VATS and identified cancer cells at margins in canine models of lung cancer(6).

We discovered intraoperative molecular imaging using a targeted tracer for folate receptor alpha was exquisitely sensitive for lung adenocarcinomas and ground glass opacities(9, 25). It can be administered 2 to 12 hours prior to surgery, and several thoroscopes can detect the tracer. Human studies using the folate-derived contrast agent showed how to optimize the camera(22, 25). Subsequently, pilot studies and then a Phase 1 IMI study (n=20 patients) showed safety and minimal toxicity(11). Synchronous malignancies were discovered in non-operative lobes during routine pulmonary resections. Intraoperative molecular imaging was also useful in identifying malignant ground glass opacities when the preoperative tissue diagnosis was unknown(3, 10), and provided information to the surgeon beyond that from PET images and frozen section. Intraoperative molecular imaging was not clinically useful for locating positive lymph nodes because of the false positive rate secondary to dye uptake on folate receptor beta on activated macrophages.

Our multi-institutional Phase 2 study presents several important points which expand on our previous findings.

First, despite preoperative 1 mm CT scans and PET scans on all patients, IMI alone identified 7 primary adenocarcinomas, 1 metastatic adenocarcinoma from the primary cancer, and 2 metastatic papillary thyroid cancers. These lesions upstaged each patient, and in some cases changed the need for adjuvant therapy. Although 15 additional nodules were resected that were benign, the additional resection did not pose a significant morbidity. IMI is only sensitive for peripheral nodules less than 2 cm from the surface, so the additional procedures were all wedges. IMI is not useful for deeper nodules that would require a segment or a lobe. Typically, an additional wedge does not change the magnitude of the operation and protects the patient against extensive extra procedures.

At this time, no technology other than visual inspection and manual palpation is available to locate nodules that are not visible on CT scanning. Nearly ~40% of lobectomies in the US are performed minimally invasively thus further limiting the surgeons' ability to perform manual manipulation. If a synchronous lesion is missed during surgery, identifying synchronous lesions on surveillance scans is challenging because new nodules are confused radiographically with scars, effusions, lung retraction, and rounded atelectasis. It can take serial CT scans to discriminate if the nodule is a new cancer or residual from the surgery.



This is of particular importance as synchronous cancers have a worse prognosis(26–28). Improved intraoperative identification of these synchronous lesions by IMI provides an opportunity for improving long-term survival(26–28).

Second, IMI localized 11 primary tumors, 6 of which were ground glass opacities that could not be felt or seen intraoperatively. This is valuable because it avoids increasing the magnitude of the operation until the surgeon had performed a wedge or segment and obtained a frozen section for diagnosis. The 2 most common scenarios were either (a) small peripheral ground glass opacity in which a wedge was the definitive operation, or (b) the nodule was undiagnosed so a wedge had to be performed for frozen pathology.

Third, rapid back-table margin review of fluorescence identified 16 close margins, 9 of which had cancer cells within 5 mm of the staple line. In subgroup analysis, these findings were most frequent during sublobar resections for ground glass opacities. In all the cases of a positive margin, the surgeons' visual inspection proved to be inadequate. Second, IMI allowed to pinpoint the location of the positive margin for a focused frozen section examination. Third, as previously published, IMI requires less than 2 minutes whereas frozen section takes ~25 minutes. Positive surgical margins have enormous oncologic and economic implications. Having close surgical margins doubles the risk of death for the patient(29–31). In addition, each close surgical margin during pulmonary resections can cost from \$6000 to \$129,000 in additional medical costs(31). Technology to reduce positive margins can provide clear value, perhaps the most important value added by IMI.

In this study, we defined close margins as tumor within 5 mm of the staple line. We chose this distance based on the propensity of tissue to collect and distort within the staple line itself. Using this criterion, 8 patients had a close margin identified by IMI. In 5 cases, the surgeon took additional tissue by additional wedge or completion lobectomy. The immediate fluorescent feedback provided by IMI was able to increase surgeon confidence when close margins were a concern, particularly in the case of ground-glass opacities which often display subtle or no changes. Therefore, the negative predictive value is an important use of IMI.

This Phase 2 study revealed several issues that deserve further attention. First, we used multiple camera systems at different sites—this included slightly different excitation and detection configurations, different scope sizes, and angles. Most surgeons found signal more robust when using a 0-degree scope, as this allows for maximum fluorescent detection. Second, depth of penetration remains an issue, and IMI is likely applicable only to lesions located within 2–3cm of the pleural surface. Third, IMI displays a high false positive rate in the lymph nodes. Fourth, IMI has limited utility near the hilum due to high levels of autofluorescence in the 800nm range(22).

IMI improved outcomes for 26% of patients undergoing pulmonary resection for NSCLC. We believe IMI provides a useful adjunct during pulmonary resections. A multi-institutional, randomized Phase 3 clinical trial evaluating IMI is underway(32).



## References

1. Predina JD, Newton AD, Connolly C et al. Identification of a folate receptor-targeted near-infrared molecular contrast agent to localize pulmonary adenocarcinomas. *Mol Ther* 2018;26(2):390–403. [PubMed: 29241970]
2. Newton AD, Predina JD, Nie S, Low PS, Singhal S. Intraoperative fluorescence imaging in thoracic surgery. *J Surg Oncol* 2018.
3. Predina JD, Newton AD, Keating J et al. Intraoperative molecular imaging combined with positron emission tomography improves surgical management of peripheral malignant pulmonary nodules. *Ann Surg* 2017;266(3):479–488. [PubMed: 28746152]
4. Rogalla S, Joosten SCM, Alam IS, Gambhir SS, Vermesh O. Intraoperative molecular imaging in lung cancer: The state of the art and the future. *Mol Ther* 2018;26(2):338–341. [PubMed: 29398484]
5. Predina JD, Fedor D, Newton AD et al. Intraoperative molecular imaging: The surgical oncology's north star. *Ann Surg* 2017.
6. Keating JJ, Runge JJ, Singhal S et al. Intraoperative near-infrared fluorescence imaging targeting folate receptors identifies lung cancer in a large-animal model. *Cancer* 2017;123(6):1051–1060. [PubMed: 28263385]
7. Okusanya OT, Holt D, Heitjan D et al. Intraoperative near-infrared imaging can identify pulmonary nodules. *Ann Thorac Surg* 2014.
8. Madajewski B, Judy BF, Mouchli A et al. Intraoperative near-infrared imaging of surgical wounds after tumor resections can detect residual disease. *Clin Cancer Res* 2012;18(20):5741–5751. [PubMed: 22932668]
9. Predina JD, Newton A, Corbett C et al. Localization of pulmonary ground-glass opacities with folate receptor-targeted intraoperative molecular imaging. *J Thorac Oncol* 2018;13(7):1028–1036. [PubMed: 29626619]
10. Kennedy GT, Okusanya OT, Keating JJ et al. The optical biopsy: A novel technique for rapid intraoperative diagnosis of primary pulmonary adenocarcinomas. *Ann Surg* 2015;262(4):602–609. [PubMed: 26366539]
11. Predina JD, Newton AD, Keating J et al. A phase I clinical trial of targeted intraoperative molecular imaging for pulmonary adenocarcinomas. *Ann Thorac Surg* 2018;105(3):901–908. [PubMed: 29397932]
12. Predina JD, Newton AD, Corbett C et al. A clinical trial of tumorglow to identify residual disease during pleurectomy and decortication. *Ann Thorac Surg* 2019;107(1):224–232. [PubMed: 30028985]
13. Keating JJ, Nims S, Venegas O et al. Intraoperative imaging identifies thymoma margins following neoadjuvant chemotherapy. *Oncotarget* 2016;7(3):3059–3067. [PubMed: 26689990]
14. Kennedy GT, Newton A, Predina J, Singhal S. Intraoperative near-infrared imaging of mesothelioma. *Transl Lung Cancer Res* 2017;6(3):279–284. [PubMed: 28713673]
15. Newton AD, Predina JD, Corbett CJ et al. Optimization of second window indocyanine green for intraoperative near-infrared imaging of thoracic malignancy. *J Am Coll Surg* 2019;228(2):188–197. [PubMed: 30471345]
16. Newton AD, Predina JD, Frenzel-Sulyok LG, Shin MH, Wang Y, Singhal S. Intraoperative near-infrared imaging can identify sub-centimeter colorectal cancer lung metastases during pulmonary metastasectomy. *J Thorac Dis* 2018;10(7):E544–E548. [PubMed: 30174930]
17. Predina JD, Keating J, Newton A et al. A clinical trial of intraoperative near-infrared imaging to assess tumor extent and identify residual disease during anterior mediastinal tumor resection. *Cancer* 2019;125(5):807–817. [PubMed: 30561757]
18. Predina JD, Newton A, Corbett C et al. A brief report: Localization of pulmonary ground-glass opacities with folate receptor-targeted intraoperative molecular imaging. *J Thorac Oncol* 2018.
19. Predina JD, Newton AD, Corbett C et al. Near-infrared intraoperative imaging for minimally invasive pulmonary metastasectomy for sarcomas. *The Journal of Thoracic and Cardiovascular Surgery* 2019;157(5):2061–2069. [PubMed: 31288365]

20. Predina JD, Newton AD, Desphande C, Singhal S. Near-infrared intraoperative imaging during resection of an anterior mediastinal soft tissue sarcoma. *Mol Clin Oncol* 2018;8(1):86–88. [PubMed: 29387401]
21. Predina JD, Newton AD, Xia L et al. An open label trial of folate receptor-targeted intraoperative molecular imaging to localize pulmonary squamous cell carcinomas. *Oncotarget* 2018;9(17):13517–13529. [PubMed: 29568374]
22. Predina JD, Okusanya O, A DN, Low P, Singhal S. Standardization and optimization of intraoperative molecular imaging for identifying primary pulmonary adenocarcinomas. *Mol Imaging Biol* 2018;20(1):131–138. [PubMed: 28497233]
23. De Jesus E, Keating JJ, Kularatne SA et al. Comparison of folate receptor targeted optical contrast agents for intraoperative molecular imaging. *Int J Mol Imaging* 2015;2015:469047. [PubMed: 26491562]
24. O'Shannessy DJ, Yu G, Smale R et al. Folate receptor alpha expression in lung cancer: Diagnostic and prognostic significance. *Oncotarget* 2012.
25. Predina JD, Newton A, Connolly C, Singhal S. Folate receptor-targeted molecular imaging improves identification of malignancy during pulmonary resection: A case report. *J Cardiothorac Surg* 2017;12(1):110. [PubMed: 29202877]
26. Cheng H, Lei BF, Peng PJ, Lin YJ, Wang XJ. Histologic lung cancer subtype differentiates synchronous multiple primary lung adenocarcinomas from intrapulmonary metastases. *J Surg Res* 2017;211:215–222. [PubMed: 28501120]
27. Okada M, Tsubota N, Yoshimura M, Miyamoto Y. Operative approach for multiple primary lung carcinomas. *J Thorac Cardiovasc Surg* 1998;115(4):836–840. [PubMed: 9576219]
28. Shrager JB. Approach to the patient with multiple lung nodules. *Thorac Surg Clin* 2013;23(2):257–266. [PubMed: 23566977]
29. Hancock JG, Rosen JE, Antonicelli A et al. Impact of adjuvant treatment for microscopic residual disease after non-small cell lung cancer surgery. *Ann Thorac Surg* 2015;99(2):406–413. [PubMed: 25528723]
30. Osarogiagbon RU, Ray MA, Faris NR et al. Prognostic value of national comprehensive cancer network lung cancer resection quality criteria. *Ann Thorac Surg* 2017;103(5):1557–1565. [PubMed: 28366464]
31. Tringale KR, Pang J, Nguyen QT. Image-guided surgery in cancer: A strategy to reduce incidence of positive surgical margins. *Wiley Interdiscip Rev Syst Biol Med* 2018;10(3):e1412. [PubMed: 29474004]
32. Elucidate trial. Available at <https://clinicaltrials.gov/ct2/show/NCT04241315?term=OTL38&draw=2&rank=5>.

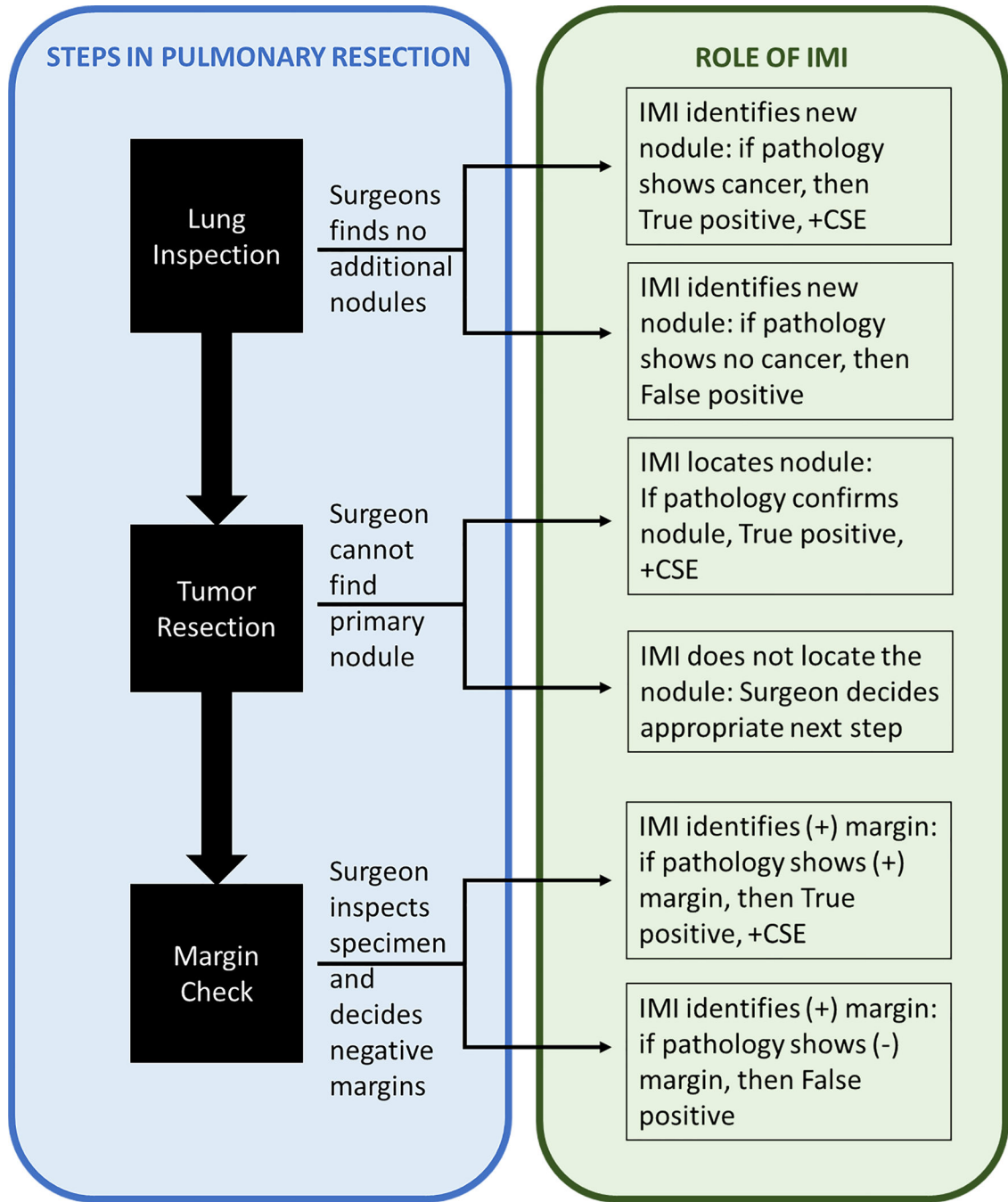


**Figure 1:** Utilization of Intraoperative Molecular Imaging (IMI) during standard steps of a pulmonary resection


**CONSORT**  
 TRANSPARENT REPORTING of TRIALS  
 CONSORT 2010 Flow Diagram

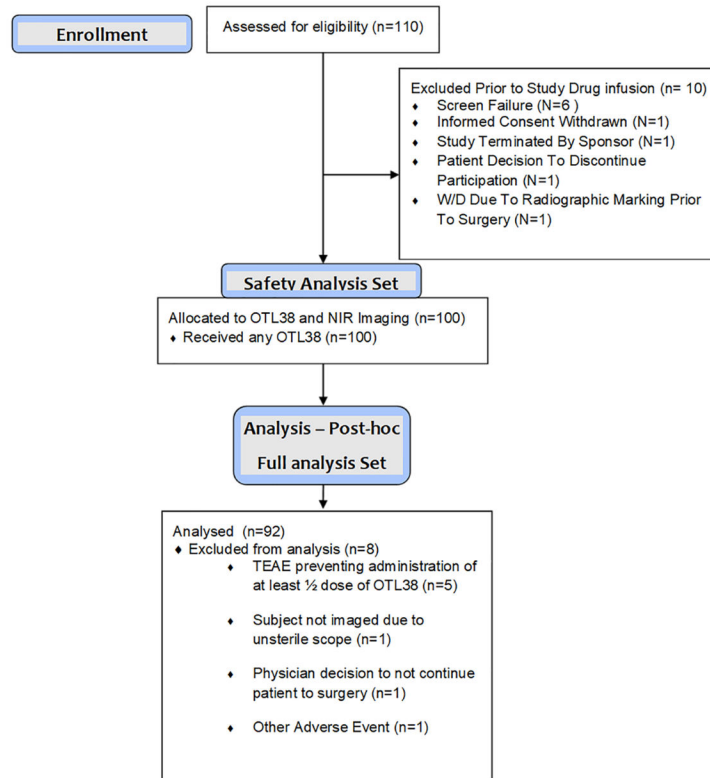


**Figure 2:**  
CONSORT diagram.

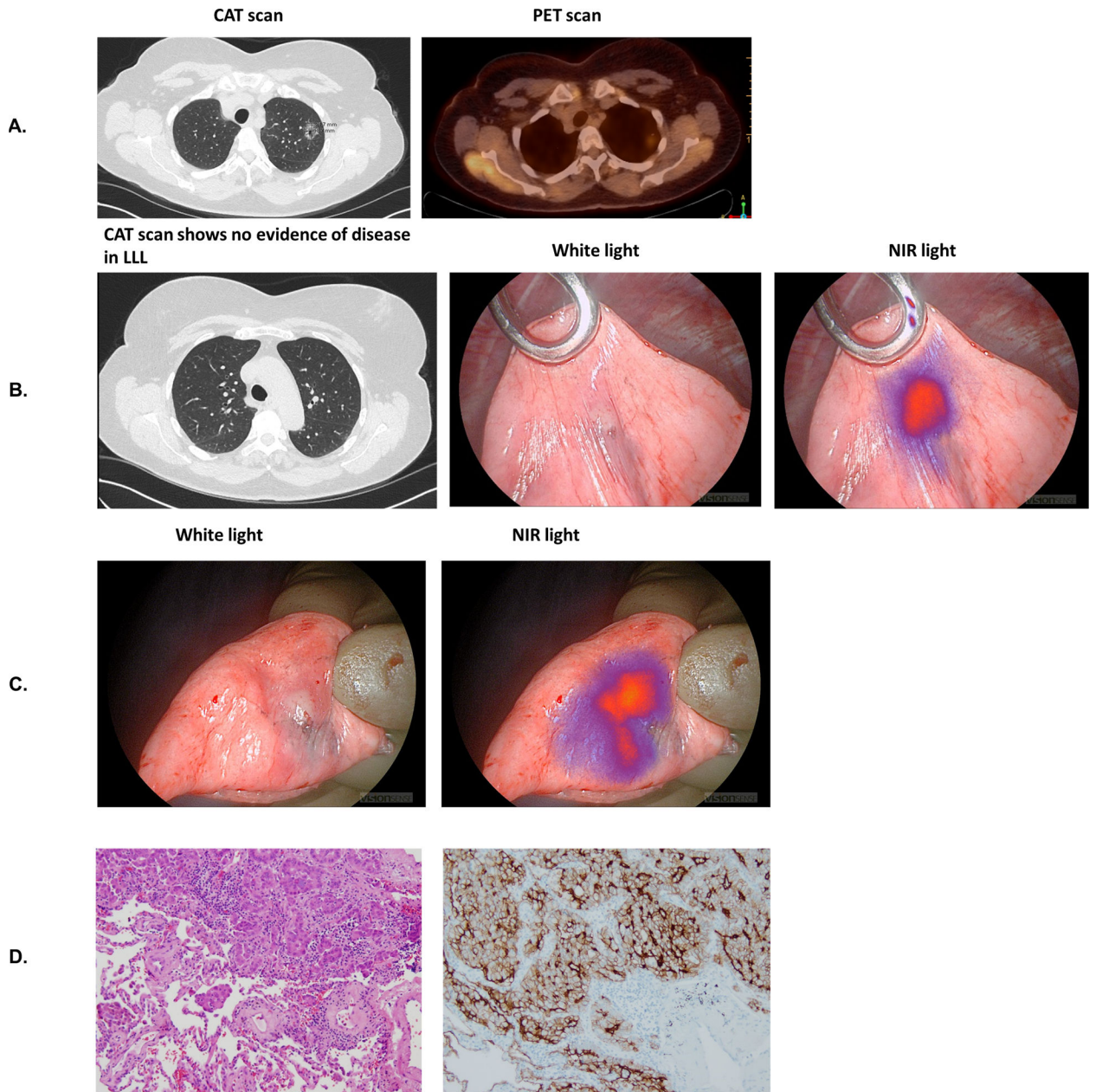


**Figure 3:**  
Synchronous Lesion clinically significant event. 1a) Known LUL pulmonary nodule on CAT/PET scan. 1b) Incidental LUL pulmonary nodule. 1c) Excised LLL pulmonary nodule. 1d) H&E and FR- $\alpha$  immunohistochemistry.



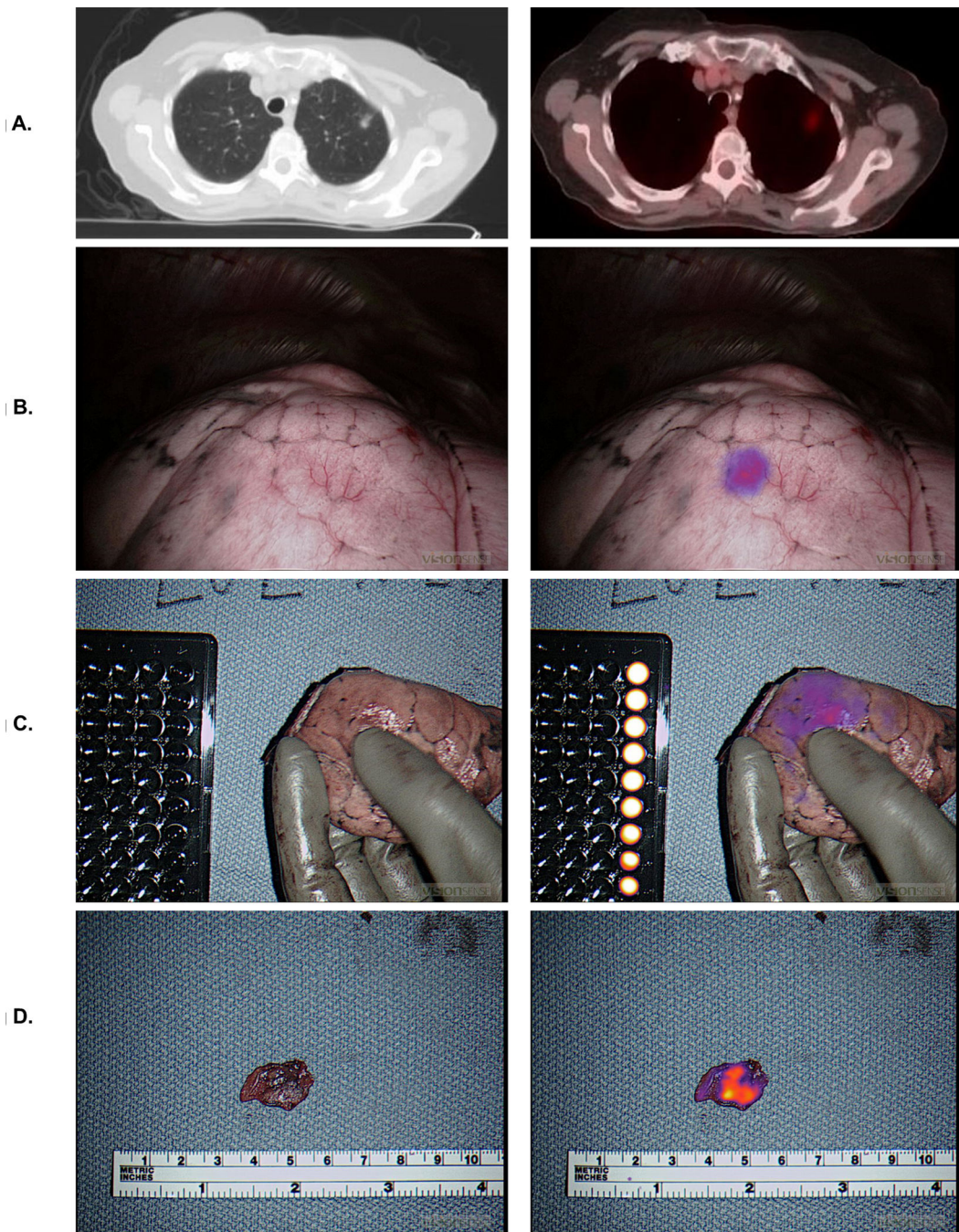


**Figure 4:**  
Localization clinically significant event. 2a) LUL ground glass opacity on CAT scan and PET scan. 2b) Intraoperative localization using Intraoperative Molecular Imaging. 2c) Ex vivo image of lung wedge. 2d) Ex vivo imaging of slice of lung nodule.

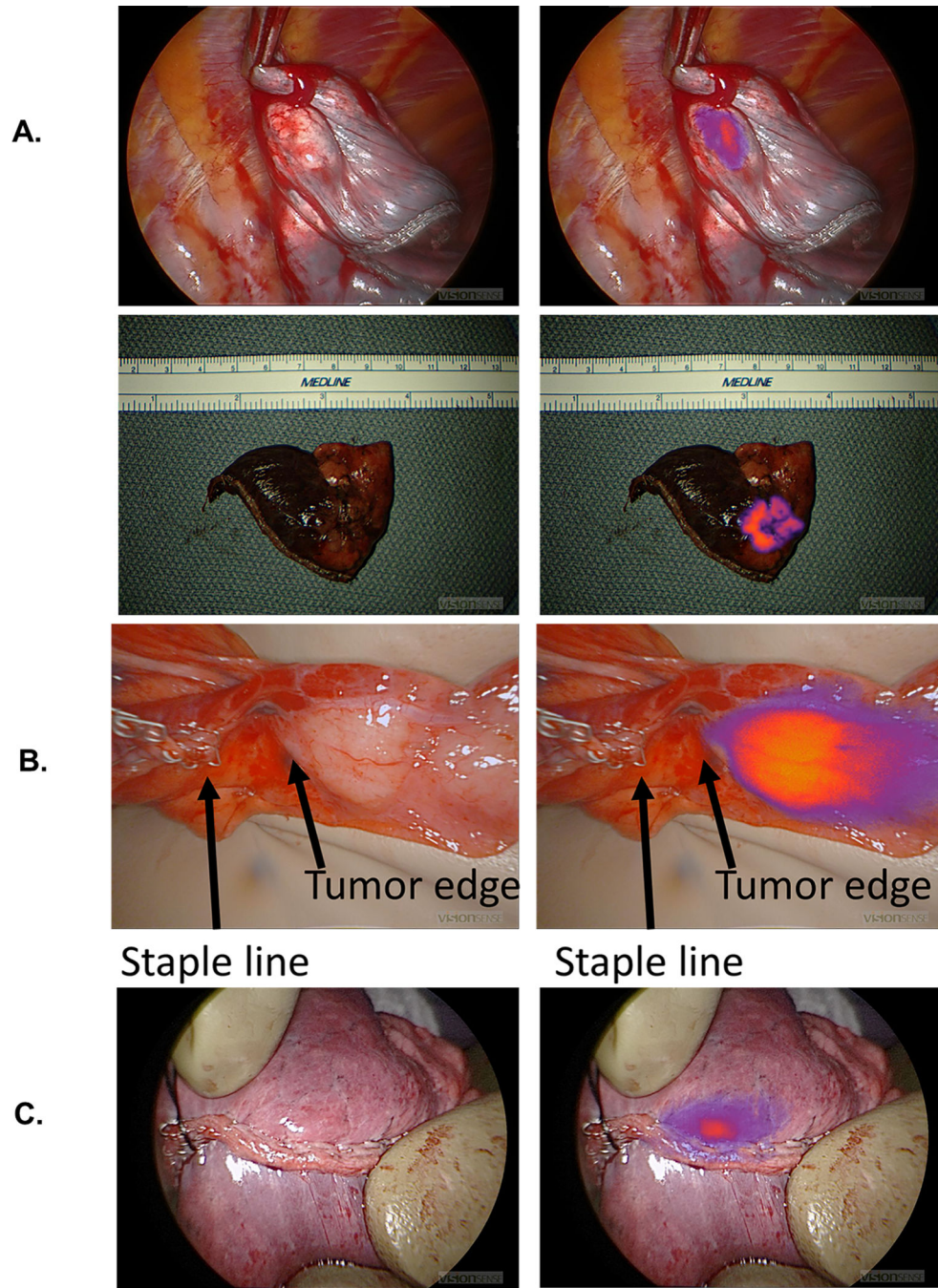


**Figure 5:** Margins clinically significant event. 3a) Example of negative margins. 3b) Example of close margins on back-table analysis. 3c) Example of positive margins on back-table analysis.



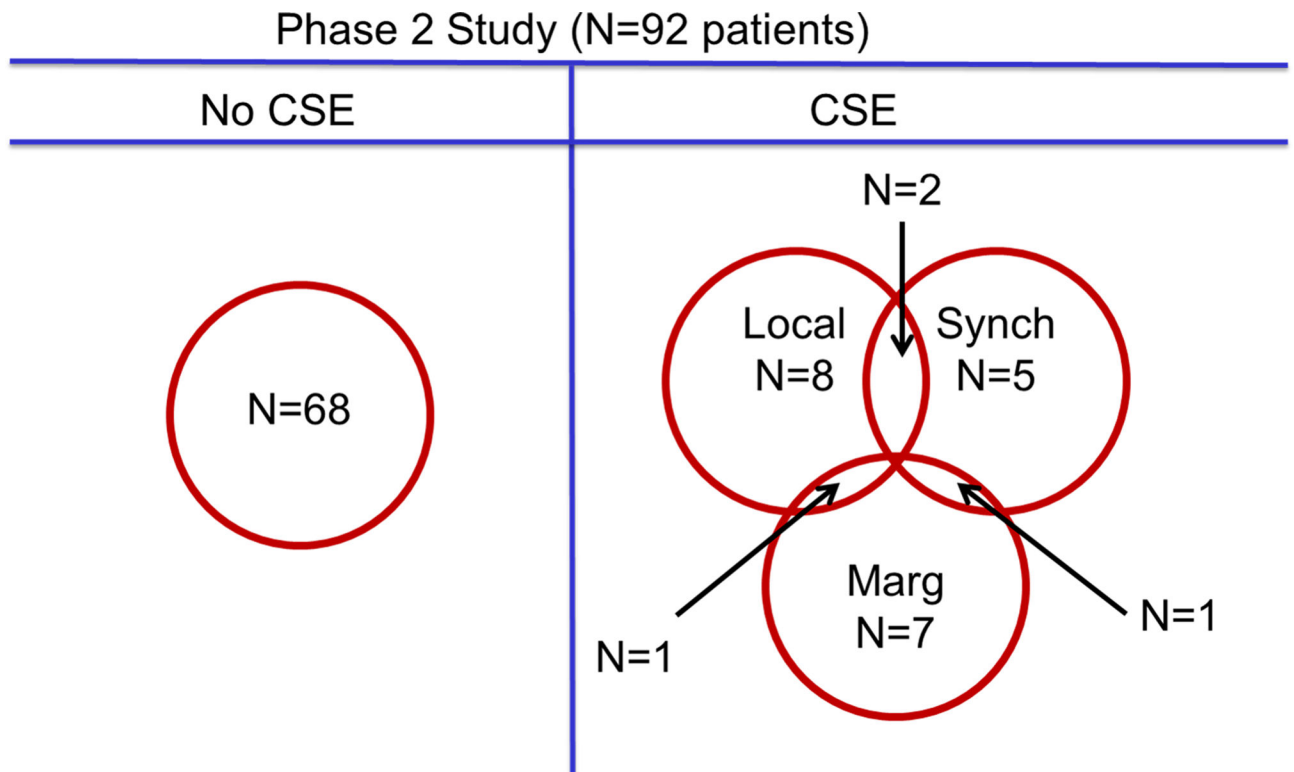


**Figure 6:**  
Clinical significant events

**Table 1:**

## Summary of Patient Characteristics

		Data
	Preoperative diagnosis of non-small cell lung cancer	43 (45%)
	Preoperative tumor size based on CT imaging (cm)	2.27 (SD 1.8, min 0.5, max 12.5)
	Total patients enrolled	110
	Patients excluded from analysis	10
	Female	68
	Final diagnosis not cancer	8
	Total patients analyzed	92
	Mean Age	67.4 (SD 9.4, Min 31, max 86)
Toxicity		
	Grade 1	36
	Grade 2	18
	Grade 3	2
Surgical procedures		
	Wedge	64
	Segmentectomy	16
	Lobectomy	43
	Bi-lobectomy	2
	Pneumonectomy	1
Pathology		
	Adenocarcinoma	64
	non-Adenocarcinoma	18
	Benign	10

**Table 2:**

## Clinically Significant Events

	Data
<b>Total number of patients analyzed</b>	92 patients
<b>Synchronous nodules</b>	
Synchronous nodules identified only by IMI	24 nodules
Cancerous synchronous nodules identified only by IMI	9 nodules
Number of patients with synchronous nodules identified only IMI	7 patients
Number of patients with change in clinical stage due to IMI	7 patients
<b>Additional cancers discovered by IMI</b>	
Stage IA adenocarcinoma	6 patients
Adenoid cystic carcinoma	1 patient
Stage IV papillary thyroid cancer	1 patient
<b>Tumor localization</b>	
Localization of primary pulmonary nodule only by IMI	11 patients
<b>Margin identification</b>	
Close margins (<5 mm) detected by IMI	16 patients
True positive margin	9 patients
<b>Summary of clinically significant events</b>	
Total number of clinically significant events	28
Number of patients with change in clinical stage due to IMI	7 patients
Total number of patients with clinically significant events	24
Percent of patients with clinically significant events	26%

IMI = Intraoperative molecular imaging